

## $t$ expansion of QCD baryons

D. Schreiber

*School of Physics and Astronomy, Raymond and Beverly Sackler Faculty of Exact Sciences,  
Tel Aviv University, Tel Aviv 69978, Israel*

(Received 11 June 1993)

We use the  $t$ -expansion method to calculate the baryonic spectrum of Hamiltonian lattice QCD with two massless dynamical quarks within the Kogut-Susskind formulation. We find this two-flavor model to possess three baryonic irreducible representations. Restricting ourselves to zero-momentum lattice states which are generated by an elementary cube, we calculate the masses of the  $\Delta$  and the  $J^P = \frac{1}{2}^-$  nucleon, and then study the scaling ratios of these particles with the lowest-lying hadrons which we have previously calculated, i.e., the  $\omega$  meson, the  $0^{++}$ , and the nucleon. On the basis of an  $H^7$  expansion we find the  $\Delta$  and the  $\frac{1}{2}^-$  nucleon to be 25 % heavier than their observed values.

PACS number(s): 12.38.Gc, 11.15.Ha, 14.20.Gk

### I. INTRODUCTION

In this paper we employ the  $t$  expansion to calculate the baryon spectrum of lattice QCD within the Kogut-Susskind formulation, using a Hamiltonian of two massless dynamical quarks. This work follows a recent publication [1] where we have calculated masses of the lowest-lying hadrons.

Our lattice QCD calculation differs from the widespread Monte Carlo simulations in two features. First, our calculations are analytical rather than numerical. Second, we work with two flavors, in contrast with the standard Lagrangian approach that deals with four flavors. The four-flavor model has an extra U(1) continuous chiral symmetry which, when spontaneously broken, yields a massless pion. In order to avoid finite-size effects connected with the massless pion [2], one has to work with nonzero quark masses. In contrast, the two-flavor formulation has only a discrete chiral symmetry, and hence lacks a Goldstone boson. Nonetheless note that it allows working with massless quarks in a confining theory.

In a previous publication [1], we have calculated the masses of the scalar state  $0^{++}$ , the nucleon, and the lowest-lying mesons, i.e.,  $\rho$ ,  $\omega$ , and  $\pi$ . On the basis of an  $H^7$  expansion, we found the mesons to be completely degenerate. The high mass of the pion was connected to the lack of continuous chiral symmetry in our model. The ratio of  $N$  to  $\omega$  turned out to be of the right magnitude, i.e., 1.2–1.5.

Any attempt at calculating masses of hadrons heavier than the lowest-lying mesons or the nucleon necessitates further understanding of the particle content of higher lattice states. Such a group-theoretical analysis was carried out by Golterman and co-worker [3,4] for the case of four flavors. We have repeated the analysis for the two-flavor zero-momentum case. The two-flavor model possesses three baryonic irreducible representations (irreps), designated as **4**, **4'**, and **8**. In the positive parity sector, the irrep **4** corresponds to the continuum nucleon,

while the other two irreps yield the  $\Delta$  state. In the negative-parity sector, these irreps correspond to the  $\frac{1}{2}^-$ ,  $\frac{5}{2}^-$ , and  $\frac{3}{2}^-$  nucleon, respectively. Limiting ourselves to zero-momentum lattice states which are generated by an elementary cube, we are able to compute the lowest  $\frac{3}{2}^+\Delta$  and  $\frac{1}{2}^-$  nucleon states.

The article is organized as follows. In Secs. II and III we briefly review the Kogut-Susskind formulation and the symmetry operations of the Hamiltonian. In Sec. IV we analyze the structure of the two-flavor symmetry group. In Sec. V we find the correspondence between the baryonic representations of the lattice and continuum QCD. In Sec. VI we build the lattice baryon states. In Sec. VII we briefly describe the  $t$ -expansion method, and in Sec. VIII we calculate the  $\Delta$  and the excited nucleon. Section IX contains a discussion of the results.

### II. THE KOGUT-SUSSKIND HAMILTONIAN

The SU(3) pure gauge theory as defined by the Kogut-Susskind Hamiltonian is [5]

$$H_G = \frac{g^2}{2} \left[ \sum_l E_l^2 + x \sum_p (6 - \text{tr} U_p - \text{tr} U_p^\dagger) \right], \quad (2.1)$$

where  $g$  is the coupling constant and  $x = 2/g^4$ . The link operators  $E_l$  and  $U_l$  which appear in Eq. (2.1) are conjugate quantum variables satisfying the commutation relations

$$[E_l^a, U_{l'}] = \frac{\lambda^a}{2} U_l \delta_{ll'}, \quad (2.2)$$

where  $\lambda^a$  are the eight Gell-Mann matrices of SU(3).  $E_l^a$  is the color electric flux operator associated with the link  $l$ , and  $\text{tr} U_p$  is the color magnetic flux operator associated with the plaquette  $p$ .

For dynamical fermions we employ the Kogut-Susskind scheme [6–9] in which the fermions are represented by a single degree of freedom per site,

$$\{\chi_i^\dagger(\mathbf{r}), \chi_j(\mathbf{r}')\} = \delta_{\mathbf{r},\mathbf{r}'} \delta_{ij}, \quad (2.3)$$

where  $i, j$  are color indices. The fermionic part of the Hamiltonian is

$$H_F = \frac{i}{2} \sum_{\mathbf{r}, \mu} \eta_\mu(\mathbf{r}) [\chi^\dagger(\mathbf{r}) U(\mathbf{r}, \mu) \chi(\mathbf{r} + \mu) - \chi^\dagger(\mathbf{r} + \mu) U^\dagger(\mathbf{r}, \mu) \chi(\mathbf{r})], \quad (2.4)$$

where

$$\eta_x(\mathbf{r}) = (-1)^z, \quad \eta_y(\mathbf{r}) = (-1)^x, \quad \eta_z(\mathbf{r}) = (-1)^y, \quad (2.5)$$

$\mathbf{r}$  varies over the lattice sites, and  $\mu$  over the three directions of space.  $H_F$  describes QCD with two massless quarks ( $u$  and  $d$ ).

Starting with the strong-coupling vacuum  $|0\rangle$ , which is the state annihilated by the color electric field

$$\mathbf{E}_l |0\rangle = 0, \quad (2.6)$$

we realize that it will lead to high degeneracy in lowest order of strong coupling since  $H_F$  will have vanishing expectation values irrespective of the choices made for the fermion occupation number,

$$\rho(\mathbf{r}) = [\chi^\dagger(\mathbf{r}), \chi(\mathbf{r})], \quad (2.7)$$

on any lattice site. This degeneracy is lifted only in second order in  $1/g^2$ . Thus working with our Hamiltonian  $H_F$ , one finds that in the gluonic vacuum  $|0\rangle$  it takes the effective form

$$\frac{g^2}{16} \sum_{\mathbf{r}, \mu} \rho(\mathbf{r}) \rho(\mathbf{r} + \mu) \quad (2.8)$$

in second order of the strong-coupling perturbation theory.

A color singlet state which is annihilated by  $\chi_a$  is an eigenstate of  $\rho$  with eigenvalue  $-3$ . It spans a set of eight states on every lattice site:

$$\begin{aligned} |-\rangle, |i\rangle &= \chi_i^\dagger |-\rangle, \quad |\bar{k}\rangle = \frac{1}{2} \epsilon_{ijk} \chi_i^\dagger \chi_j^\dagger |-\rangle, \\ |+\rangle &= \frac{1}{6} \epsilon_{ijk} \chi_i^\dagger \chi_j^\dagger \chi_k^\dagger |-\rangle. \end{aligned} \quad (2.9)$$

The first and the last are color singlets corresponding to  $\rho$  eigenvalues of  $-3$  and  $3$ , respectively. The others are color triplets and antitriplets with eigenvalues of  $-1$  and  $1$ .

The trial vacuum is chosen in a staggered form which divides the lattice into two sublattices, that of even  $r$  (i.e., even  $x+y+z$ ) and that of odd  $r$ :

$$|v\rangle = \Pi_{\text{odd } \mathbf{r}} |+\rangle \Pi_{\text{even } \mathbf{r}} |-\rangle |0\rangle. \quad (2.10)$$

Thus we have chosen the  $\chi^\dagger(\chi)$  to reside on even (odd) sites. Since our discrete chiral transformations take even (odd) sites into odd (even) sites, chiral symmetry is spontaneously broken.

### III. TWO-FLAVOR HAMILTONIAN SYMMETRY GROUP

The two-flavor fermionic Hamiltonian possesses the following symmetries.

#### A. Even translations

For even translations, we have

$$\chi(\mathbf{r}) \rightarrow \chi(\mathbf{r} + 2\mathbf{r}_0), \quad U(\mathbf{r}, \mu) \rightarrow U(\mathbf{r} + 2\mathbf{r}_0, \mu), \quad (3.1)$$

where  $\mathbf{r}_0$  has integer components. This symmetry may be interpreted as spatial translation invariance.

#### B. Odd shift invariance

For odd shift invariance, we have

$$\chi(\mathbf{r}) \rightarrow -(-1)^x \chi(\mathbf{r} + \hat{\mathbf{z}}), \quad U(\mathbf{r}, \mu) \rightarrow U(\mathbf{r} + \hat{\mathbf{z}}, \mu), \quad (3.2)$$

$$\chi(\mathbf{r}) \rightarrow -(-1)^y \chi(\mathbf{r} + \hat{\mathbf{x}}), \quad U(\mathbf{r}, \mu) \rightarrow U(\mathbf{r} + \hat{\mathbf{x}}, \mu), \quad (3.3)$$

$$\chi(\mathbf{r}) \rightarrow -(-1)^z \chi(\mathbf{r} + \hat{\mathbf{y}}), \quad U(\mathbf{r}, \mu) \rightarrow U(\mathbf{r} + \hat{\mathbf{y}}, \mu). \quad (3.4)$$

These transformations are the discrete remnant of the chiral  $SU(2)_V \times SU(2)_A$  which the continuum theory of two massless quarks possesses. In the naive continuum limit they become, respectively,

$$q \rightarrow \gamma_5 \tau_3 q, \quad (3.5)$$

$$q \rightarrow \gamma_5 \tau_1 q, \quad (3.6)$$

$$q \rightarrow \gamma_5 \tau_2 q. \quad (3.7)$$

Combining three successive transformations, we obtain a shift along a main diagonal of a cube,

$$\chi(\mathbf{r}) \rightarrow -(-1)^{x+y+z} \chi(\mathbf{r} + \hat{\mathbf{x}} + \hat{\mathbf{y}} + \hat{\mathbf{z}}), \quad (3.8)$$

which can be identified in the continuum limit as the chiral transformation

$$q \rightarrow i\gamma_5 q. \quad (3.9)$$

#### C. "Face" diagonal shifts

Since the odd shift transformations take even (odd) sites into odd (even) sites, they are spontaneously broken by the strong coupling vacuum. However, if we apply two such odd shifts successively, we obtain shifts along "face" diagonals, which are not broken:

$$\chi(\mathbf{r}) \rightarrow -(-1)^y \chi(\mathbf{r} + \hat{\mathbf{x}} + \hat{\mathbf{y}}), \quad (3.10)$$

$$\chi(\mathbf{r}) \rightarrow -(-1)^z \chi(\mathbf{r} + \hat{\mathbf{y}} + \hat{\mathbf{z}}), \quad (3.11)$$

$$\chi(\mathbf{r}) \rightarrow -(-1)^x \chi(\mathbf{r} + \hat{\mathbf{z}} + \hat{\mathbf{x}}). \quad (3.12)$$

These shifts correspond, in the continuum limit, to isospin rotation of  $\pi$  about the  $z, x, y$  axes, respectively:

$$q \rightarrow i\tau_3 q, \quad (3.13)$$

$$q \rightarrow i\tau_1 q, \quad (3.14)$$

$$q \rightarrow i\tau_2 q. \quad (3.15)$$

#### D. Cubic lattice rotations

These rotate the lattice by  $\pi/2$  about any axis keeping the origin. Let  $\mathbf{r} \rightarrow \mathbf{r}'$  be such a rotation; then  $\chi(\mathbf{r})$  transforms as

$$i'\chi(\mathbf{r}) \rightarrow i' R(x, y, z) \chi(\mathbf{r}'), \quad U(\mathbf{r}, \mu) \rightarrow U(\mathbf{r}', \mu'), \quad (3.16)$$

where

$$U(\mathbf{r}, \mu) = \begin{cases} U(\mathbf{r}, \mu), & \mu \text{ positive,} \\ U^\dagger(\mathbf{r} + \mu, -\mu), & \mu \text{ negative,} \end{cases} \quad (3.17)$$

and

$$R(x, y, z) = \frac{1}{2} [(-1)^x + (-1)^y + (-1)^z - (-1)^{x+y+z}], \quad (3.18)$$

and  $R(x, y, z)$  satisfies  $R(x, y, z)^2 = 1$ . These transformations generate the group of rotational symmetry of a cube, the octahedral group  $O$ . Let  $\mathbf{r}'$  be obtained from  $\mathbf{r}$  by a  $\pi/2$  rotation around the  $z$ ,  $x$ , and  $y$  axes, respectively, then such a transformation corresponds, in the continuum limit, to simultaneous rotation by  $\pi/2$  in both space and isospace:

$$q(\mathbf{r}) \rightarrow \exp \left[ i \frac{\pi}{2} (J_3 + \tau_3) \right] q(\mathbf{r}'), \quad (3.19)$$

$$q(\mathbf{r}) \rightarrow \exp \left[ i \frac{\pi}{2} (J_1 + \tau_1) \right] q(\mathbf{r}'), \quad (3.20)$$

$$q(\mathbf{r}) \rightarrow \exp \left[ i \frac{\pi}{2} (J_2 + \tau_2) \right] q(\mathbf{r}'). \quad (3.21)$$

Rotating by  $\pi$  in ordinary space can be compounded by applying twice a cubic rotation and then undoing the isospin rotation by a face diagonal shift. This amounts to rotating a given cube about its geometrical center.

#### E. Parity

This is simply

$$\chi(\mathbf{r}) \rightarrow (-1)^{x+y+z} \chi(-\mathbf{r}), \quad U(\mathbf{r}, \mu) \rightarrow U^\dagger(-\mathbf{r}, \mu). \quad (3.22)$$

This corresponds, in the continuum, to

$$q \rightarrow \gamma_0 q. \quad (3.23)$$

These symmetry operations were given in Refs. [6–8]. In addition, one can think of odd shifts which will not be broken by the vacuum, as was done for the two-flavor Lagrangian [10]. In the Hamiltonian approach, this corresponds to odd shifts combined with an interchange of  $\chi$  with  $\chi^\dagger$ :

$$\chi(\mathbf{r}) \rightarrow (-1)^y \chi^\dagger(\mathbf{r} + \hat{x}), \quad U(\mathbf{r}, \mu) \rightarrow U^*(\mathbf{r} + \hat{x}, \mu), \quad (3.24)$$

$$\chi(\mathbf{r}) \rightarrow (-1)^z \chi^\dagger(\mathbf{r} + \hat{y}), \quad U(\mathbf{r}, \mu) \rightarrow U^*(\mathbf{r} + \hat{y}, \mu), \quad (3.25)$$

$$\chi(\mathbf{r}) \rightarrow (-1)^x \chi^\dagger(\mathbf{r} + \hat{z}), \quad U(\mathbf{r}, \mu) \rightarrow U^*(\mathbf{r} + \hat{z}, \mu). \quad (3.26)$$

These transformations can yield, when squared, the face diagonal even shifts. But, since these transformations involve interchanging particles with antiparticles, we shall not include them in our group analysis. However, they are useful for finding an appropriate candidate for the charge-conjugation operation. In fact, we shall now show that Eq. (3.25) corresponds to the charge-conjugation operation in the continuum limit.

#### F. Charge conjugation

In order to find the lattice version of the charge-conjugation operation, we note that using our conventions, one can easily verify the following correspondence between lattice and continuum operations. The continuum operation

$$q \rightarrow (q^\dagger)^T \quad (3.27)$$

corresponds to

$$\chi(\mathbf{r}) \rightarrow (-1)^y \chi^\dagger(\mathbf{r}). \quad (3.28)$$

Moreover, the operation

$$q \rightarrow \gamma_2 q \quad (3.29)$$

corresponds to

$$\chi(\mathbf{r}) \rightarrow (-1)^{y+z} \chi(\mathbf{r} + \hat{y}). \quad (3.30)$$

Combining these operations, we obtain the lattice charge conjugation:

$$\chi(\mathbf{r}) \rightarrow (-1)^z \chi^\dagger(\mathbf{r} + \hat{y}). \quad (3.31)$$

#### G. G parity

$G$  parity is obtained by supplementing our charge conjugation with an isospin rotation of  $\pi$  along the  $y$  axis:

$$\chi(\mathbf{r}) \rightarrow -(-1)^{x+y+z} \chi^\dagger(\mathbf{r} + \hat{x} + \hat{y} + \hat{z}). \quad (3.32)$$

Note that this differs from the result of Ref. [8].

#### H. Baryon number conservation

This is a continuous  $U(1)$  invariance:

$$\chi(\mathbf{r}) \rightarrow e^{i\alpha} \chi(\mathbf{r}).$$

### IV. TWO-FLAVOR GEOMETRICAL REST-FRAME GROUP

Since we are interested in zero-momentum states, we concentrate on the rest-frame group having the symmetries described in Secs. III C–III H. We shall deal with sectors with well-defined quark number, thus we can ignore the  $U(1)$  symmetry. Moreover, parity and charge conjugation can be easily added to our states. Thus, our analysis reduces to the geometrical group of cubic rotations and face diagonal shifts, the group  $G(S_{ij}, R_{kl})$ , where  $S_{ij}$  is a shift along a face diagonal in the  $(ij)$  plane, and  $R_{kl}$  is a  $\pi/2$  rotation in the  $(kl)$  plane.

The shifts anticommute in the defining representation. Their squares commute and are interpreted as translations. The shifts modulo translations are interpreted as flavor transformations, as in Eqs. (3.13)–(3.15). They form an eight-element group  $S(\pm I, \pm S_{ij})$ , which is a subgroup of the  $SU(2)_{\text{flavor}}$  group of the continuum.

The rotations  $R_{ij}$  generate the octahedral group  $O$ . The 24 elements of  $O$ , enumerated in their five conjugacy classes, are as follows [11], where reference is to Cartesian coordinates  $x$ ,  $y$ , and  $z$  with the origin at the cube's

TABLE I. Character table for the irreps of the geometrical rest-frame group with two flavors.

Irreps type	Irreps name	Conjugacy classes												
		I	II	III	IV	V	VI	VII	VIII	IX	X	XI	XII	XIII
		1	6	12	1	12	24	6	32	6	32	12	24	24
Mesonic	1	1	1	1	1	1	1	1	1	1	1	1	1	1
	1'	1	1	-1	1	-1	-1	1	1	1	1	1	-1	-1
	2	2	2	0	2	0	0	2	-1	2	-1	2	0	0
	3	3	3	-1	3	-1	-1	-1	0	-1	0	-1	1	1
	3'	3	3	1	3	1	1	-1	0	-1	0	-1	-1	-1
	3''	3	-1	1	3	1	-1	3	0	-1	0	-1	1	-1
	3'''	3	-1	1	3	1	-1	-1	0	3	0	-1	-1	1
	3''''	3	-1	-1	3	-1	1	-1	0	3	0	-1	1	-1
	3'''''	3	-1	-1	3	-1	1	3	0	-1	0	-1	-1	1
	6	6	-2	0	6	0	0	-2	0	-2	0	2	0	0
Baryonic	4	4	0	2	-4	-2	0	0	1	0	-1	0	0	0
	4'	4	0	-2	-4	2	0	0	1	0	-1	0	0	0
	8	8	0	0	-8	0	0	0	-1	0	1	0	0	0

center and axes parallel to its edges:  $I$  denotes identity;  $3C_2$ ,  $\pi$  rotations about three coordinate axes;  $8C_3$ ,  $\pm(2\pi/3)$  rotations about four body diagonals, e.g.,  $x=y=z$ ;  $6C_4$ ,  $\pm(\pi/2)$  rotations about three coordinate axes;  $6C'_2$ ,  $\pi$  rotations about axes parallel to six face diagonals, e.g.,  $x=y, z=0$ .

Multiplying the elements of  $S$  with those of  $O$ , one obtains the 192 elements of  $G$ , enumerated in 13 conjugacy classes, as follows: class I contains the identity; class II contains the subgroup  $S$ ; classes III, V, and VI contain  $S \times 6C_4$ , where  $6C_4$  is contained in class III; class IV contains the negative identity for  $\pm(2\pi)$  rotations in isospace; classes VII, IX, and XI are made of  $S \times 3C_2$ , where  $3C_2$  is contained in class VII; classes VIII and X contain  $S \times 8C_3$ , where  $8C_3$  is contained in class VIII. Finally, classes XII and XIII and  $S \times 6C'_2$ , where  $6C'_2$  is contained in class XII. In Table I we display the character table of  $G$ .

The group  $G$  has two types of irreducible representations (irreps): mesonic, in which the shifts commute, and baryonic, in which they anticommute. All meson representations, where the shifts commute, are also representations of a smaller group. This smaller group has 96 elements in 10 conjugacy classes. We conclude, therefore, that the group  $G$  has three baryonic irreps and ten mesonic ones. In this paper we concentrate solely on the baryonic irreps.

## V. BARYONIC IRREPS

The defining representation is the one according to which the four fields  $\chi^\dagger(\chi)$  sitting on even (odd) sites of an elementary cube transform. The other two baryonic irreps are of dimensions 4 and 8. We denote the three irreps as  $4$ ,  $4'$ , and  $8$ , respectively.

The general form of a baryonic operator of zero momentum which is generated by an elementary cube is

$$B = \sum_{\{\text{cubes}\}} \epsilon_{ijk} \chi_i^\dagger(\mathbf{r}_1) \chi_j^\dagger(\mathbf{r}_2) \chi_k^\dagger(\mathbf{r}_3), \quad (5.1)$$

where  $\mathbf{r}_1$ ,  $\mathbf{r}_2$ , and  $\mathbf{r}_3$  are even sites within the same elementary cube. Gauge fields will be added later to make the operators locally invariant. Similarly we can build the local antibaryons from the  $\chi$  fields.  $B$  should transform as the totally symmetric part of the  $4 \times 4 \times 4$  representation of  $G$ , where we have the decomposition

$$[4 \times 4 \times 4]_{\text{symmetric}} = 2 \times 4 + 4' + 8. \quad (5.2)$$

In order to describe baryonic operators on the lattice, we introduce in Table II the pictorial notation of the  $\chi$ 's by denoting a  $\chi^\dagger$  by a cube with a dot at the corner corresponding to this field. All possible baryon operators which are included in an elementary cube are divided into three geometrical classes. Clearly each of these classes transforms within itself under the symmetry operations of  $G$ . To make the operators gauge invariant, we put gauge fields on the shortest paths connecting the sites in the cube where the  $\chi$  fields reside. To maintain covariance, the average has to be taken over all different shortest paths. By applying rotations and shifts to the operators in Table II, one can obtain all possible baryon operators generated by the elementary cube.

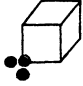
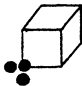
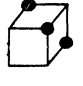
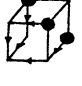
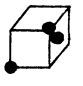
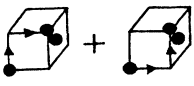
Furthermore, upon reduction of  $G$  with respect to  $O$ , we obtain

$$\begin{aligned} 4 &\rightarrow \mathbf{A}_1 + \mathbf{F}_1, \\ 4' &\rightarrow \mathbf{A}_2 + \mathbf{F}_2, \\ 8 &\rightarrow \mathbf{E} + \mathbf{F}_1 + \mathbf{F}_2. \end{aligned} \quad (5.3)$$

We observe that the baryon irreps are characterized uniquely by their  $O$  content, and hence we can find the  $4$ ,  $4'$ , and  $8$  irreps by looking for an  $\mathbf{A}_1$ ,  $\mathbf{A}_2$ , or  $\mathbf{E}$  component, respectively. The other components of  $G$  irreps can then be obtained by applying spatial rotations and shifts to the  $O$  components.

Our aim is to establish the group-theoretical relation between continuum and lattice baryon states. We consider continuum zero-momentum states with quantum num-

TABLE II. Pictorial notation for all possible baryon operators that are included in an elementary cube. A dot corresponds to a  $\chi^\dagger$  field. An arrow in the positive (negative)  $\mu$  direction denotes  $U(\mathbf{r}, \mu)$  [ $U^\dagger(\mathbf{r}, \mu)$ ].

Class	Pictorial notation	Gauge invariant operator
1		
2		
3		

bers  $(J^P, I)$ : the first label denotes total angular momentum  $J = \frac{1}{2}, \frac{3}{2}, \frac{5}{2}$ , and parity, and  $I$  is the isospin  $I = \frac{1}{2}, \frac{3}{2}$ . One can find the reduction from the continuum  $SU(2)_{\text{spin}} \times SU(2)_{\text{flavor}}$  directly to  $G$ , by using Table I, but since the baryon irreps of  $G$  are uniquely characterized by their  $O$  content, we can simplify our task by reducing the  $(J^P, I)$  irreps with respect to the subgroup  $O$ . Since the subgroup  $O$  is contained in the diagonal subgroup  $SU(2)_{\text{diagonal}}$  of  $SU(2)_{\text{spin}} \times SU(2)_{\text{flavor}}$ , the reduction is made through the chain

$$SU(2)_{\text{spin}} \times SU(2)_{\text{flavor}} \supset SU(2)_{\text{diagonal}} \supset O_h. \quad (5.4)$$

Table III shows the reduction of some  $SO(3)$  irreps to  $O$ . In Table IV we display the reduction of Eq. (5.4). Using Table IV we can find the relation between the irreps of  $G$  and the particles in the continuum. This is displayed in Table V.

Under the assumption that the ground states of lattice irreps go to the lightest state in the continuum limit, we conclude that in the positive parity sector, the irrep 4 may be used to calculate the nucleon state, while the other two irreps, 4' and 8, correspond to the  $\Delta$  particle. In the negative parity sector, we have three distinct nucleonic lightest states, namely, the  $\frac{1}{2}^-, \frac{5}{2}^-,$  and  $\frac{3}{2}^-$ , respective-

TABLE III. Reduction of  $SO(3)$  irreps with respect to the group  $O$ .

$SO(3)$	$O$	irreps
0	$\rightarrow$	$A_1$
1	$\rightarrow$	$F_1$
2	$\rightarrow$	$E + F_2$
3	$\rightarrow$	$A_2 + F_1 + F_2$
4	$\rightarrow$	$A_1 + E + F_1 + F_2$

ly. They correspond to the  $N(1535)$ ,  $N(1675)$ , and  $N(1520)$  states.

## VI. LATTICE BARYON STATES

Using the cubic lattice rotations of Eq. (3.16), one can generate the 24 elements of the octahedral group  $O$ . Starting with any baryon state  $\Psi$  from Table II, one can obtain the basis for the representation  $\mu$  of  $O$ ,  $\Psi_i^{(\mu)}$ , by applying the projection operator

$$\Psi_i^{(\mu)} = \frac{n_\mu}{g} \sum_R D_{ii}^{*(\mu)}(R) O_R \Psi, \quad (6.1)$$

where  $n_\mu$  is the dimension of the representation  $\mu$ ,  $g$  is the group size,  $D_{ii}^{(\mu)}(R)$  the matrix element of  $R \in O$  in the representation  $\mu$ , and  $O_R$  is the operator corresponding to  $R$ .

In the positive parity sector we find that the operators of class 1 in Table II are pure  $A_1^+$  states, while class 2 operators are pure  $A_2^+$  states. The third class operators can be projected both onto  $A_1^+$  and  $E^+$ . On the other hand, in the negative parity sector, the only state that can be built out of operators which are included in an elementary cube is the  $A_1^-$  state. This is achieved by using class 2 operators.

Thus we find that the lattice nucleon can be written as the local baryon state:

$$\frac{1}{6} \sum_{\mathbf{r}} \epsilon_{ijk} \chi_i^\dagger(2\mathbf{r}) \chi_j^\dagger(2\mathbf{r}) \chi_k^\dagger(2\mathbf{r}) |v\rangle. \quad (6.2)$$

This state was discussed and calculated in Ref. [1]. Another candidate for an  $A_1^+$  state is the completely symmetrized combination of class 3 operators:

$$\begin{aligned} & \frac{1}{\sqrt{48}} \sum_{\mathbf{r}} \sum_{\epsilon_1, \epsilon_2} \sum_{\{U\}} \{ \epsilon_{ijk} \chi_i^\dagger(2\mathbf{r} + \epsilon_1 \hat{x} + \epsilon_2 \hat{y}) \chi_j^\dagger(2\mathbf{r} + \epsilon_1 \hat{x} + \epsilon_2 \hat{y}) [U(2\mathbf{r} + \epsilon_1 \hat{x} + \epsilon_2 \hat{y}, 2\mathbf{r}) \chi_k^\dagger(2\mathbf{r})]_k \\ & + \epsilon_{ijk} \chi_i^\dagger(2\mathbf{r} + \epsilon_1 \hat{y} + \epsilon_2 \hat{z}) \chi_j^\dagger(2\mathbf{r} + \epsilon_1 \hat{y} + \epsilon_2 \hat{z}) [U(2\mathbf{r} + \epsilon_1 \hat{y} + \epsilon_2 \hat{z}, 2\mathbf{r}) \chi_k^\dagger(2\mathbf{r})]_k \\ & + \epsilon_{ijk} \chi_i^\dagger(2\mathbf{r} + \epsilon_1 \hat{z} + \epsilon_2 \hat{x}) \chi_j^\dagger(2\mathbf{r} + \epsilon_1 \hat{z} + \epsilon_2 \hat{x}) [U(2\mathbf{r} + \epsilon_1 \hat{z} + \epsilon_2 \hat{x}, 2\mathbf{r}) \chi_k^\dagger(2\mathbf{r})]_k \} |v\rangle, \end{aligned} \quad (6.3)$$

where  $\epsilon_1, \epsilon_2 = \pm 1$ ,  $U(\mathbf{r}_1, \mathbf{r}_2)$  indicates a shortest path of gauge links connecting sites  $\mathbf{r}_1$  and  $\mathbf{r}_2$ , and  $\sum_{\{U\}}$  means summation over all possible shortest paths.

The  $\Delta$  particle is represented by the  $A_2^+$  state

TABLE IV. Reduction of  $SU(2)_{\text{spin}} \times SU(2)_{\text{flavor}}$  with respect to  $O_h$ .

$SU(2)_{\text{spin}} \times SU(2)_{\text{flavor}}$	$SU(2)_{\text{diagonal}}$	$O^\pm$
$(\frac{1}{2}^\pm, \frac{1}{2})$	0+1	$\mathbf{A}_1^\pm + \mathbf{F}_1^\pm$
$(\frac{3}{2}^\pm, \frac{1}{2})$	1+2	$\mathbf{E}^\pm + \mathbf{F}_1^\pm + \mathbf{F}_2^\pm$
$(\frac{1}{2}^\pm, \frac{3}{2})$	1+2	$\mathbf{E}^\pm + \mathbf{F}_1^\pm + \mathbf{F}_2^\pm$
$(\frac{3}{2}^\pm, \frac{3}{2})$	0+1+2+3	$\mathbf{A}_1^\pm + \mathbf{A}_2^\pm + \mathbf{E}^\pm +$ $2\mathbf{F}_1^\pm + 2\mathbf{F}_2^\pm$
$(\frac{5}{2}^\pm, \frac{1}{2})$	2+3	$\mathbf{A}_2^\pm + \mathbf{E}^\pm + \mathbf{F}_1^\pm + 2\mathbf{F}_2^\pm$
$(\frac{5}{2}^\pm, \frac{3}{2})$	1+2+3+4	$\mathbf{A}_1^\pm + \mathbf{A}_2^\pm + 2\mathbf{E}^\pm +$ $3\mathbf{F}_1^\pm + 3\mathbf{F}_2^\pm$

$$\begin{aligned} & \frac{1}{8} \sum_{\mathbf{r}} \sum_{\epsilon_1, \epsilon_2, \epsilon_3} \epsilon_{ijk} [U(2\mathbf{r} + \epsilon_1 \hat{\mathbf{x}} + \epsilon_2 \hat{\mathbf{y}} + \epsilon_3 \hat{\mathbf{z}}, 2\mathbf{r} + \epsilon_1 \hat{\mathbf{x}} + \epsilon_2 \hat{\mathbf{y}}) \chi^\dagger(2\mathbf{r} + \epsilon_1 \hat{\mathbf{x}} + \epsilon_2 \hat{\mathbf{y}})]_i \\ & \quad \times [U(2\mathbf{r} + \epsilon_1 \hat{\mathbf{x}} + \epsilon_2 \hat{\mathbf{y}} + \epsilon_3 \hat{\mathbf{z}}, 2\mathbf{r} + \epsilon_2 \hat{\mathbf{y}} + \epsilon_3 \hat{\mathbf{z}}) \chi^\dagger(2\mathbf{r} + \epsilon_2 \hat{\mathbf{y}} + \epsilon_3 \hat{\mathbf{z}})]_j \\ & \quad \times [U(2\mathbf{r} + \epsilon_1 \hat{\mathbf{x}} + \epsilon_2 \hat{\mathbf{y}} + \epsilon_3 \hat{\mathbf{z}}, 2\mathbf{r} + \epsilon_3 \hat{\mathbf{z}} + \epsilon_1 \hat{\mathbf{x}}) \chi^\dagger(2\mathbf{r} + \epsilon_3 \hat{\mathbf{z}} + \epsilon_1 \hat{\mathbf{x}})]_k |v\rangle, \end{aligned} \quad (6.4)$$

or by the  $\mathbf{E}^+$  states

$$\begin{aligned} & \frac{1}{\sqrt{32}} \sum_{\mathbf{r}} \sum_{\epsilon_1, \epsilon_2} \sum_{\{U\}} \{ \epsilon_{ijk} \chi_i^\dagger(2\mathbf{r} + \epsilon_1 \hat{\mathbf{x}} + \epsilon_2 \hat{\mathbf{y}}) \chi_j^\dagger(2\mathbf{r} + \epsilon_1 \hat{\mathbf{x}} + \epsilon_2 \hat{\mathbf{y}}) [U(2\mathbf{r} + \epsilon_1 \hat{\mathbf{x}} + \epsilon_2 \hat{\mathbf{y}}, 2\mathbf{r}) \chi^\dagger(2\mathbf{r})]_k \\ & \quad - \epsilon_{ijk} \chi_i^\dagger(2\mathbf{r} + \epsilon_1 \hat{\mathbf{y}} + \epsilon_2 \hat{\mathbf{z}}) \chi_j^\dagger(2\mathbf{r} + \epsilon_1 \hat{\mathbf{y}} + \epsilon_2 \hat{\mathbf{z}}) [U(2\mathbf{r} + \epsilon_1 \hat{\mathbf{y}} + \epsilon_2 \hat{\mathbf{z}}, 2\mathbf{r}) \chi^\dagger(2\mathbf{r})]_k \} |v\rangle, \end{aligned} \quad (6.5)$$

and

$$\begin{aligned} & \frac{1}{\sqrt{96}} \sum_{\mathbf{r}} \sum_{\epsilon_1, \epsilon_2} \sum_{\{U\}} \{ \epsilon_{ijk} \chi_i^\dagger(2\mathbf{r} + \epsilon_1 \hat{\mathbf{x}} + \epsilon_2 \hat{\mathbf{y}}) \chi_j^\dagger(2\mathbf{r} + \epsilon_1 \hat{\mathbf{x}} + \epsilon_2 \hat{\mathbf{y}}) [U(2\mathbf{r} + \epsilon_1 \hat{\mathbf{x}} + \epsilon_2 \hat{\mathbf{y}}, 2\mathbf{r}) \chi^\dagger(2\mathbf{r})]_i \\ & \quad + \epsilon_{ijk} \chi_i^\dagger(2\mathbf{r} + \epsilon_1 \hat{\mathbf{y}} + \epsilon_2 \hat{\mathbf{z}}) \chi_j^\dagger(2\mathbf{r} + \epsilon_1 \hat{\mathbf{y}} + \epsilon_2 \hat{\mathbf{z}}) [U(2\mathbf{r} + \epsilon_1 \hat{\mathbf{y}} + \epsilon_2 \hat{\mathbf{z}}, 2\mathbf{r}) \chi^\dagger(2\mathbf{r})]_j \\ & \quad - 2\epsilon_{ijk} \chi_i^\dagger(2\mathbf{r} + \epsilon_1 \hat{\mathbf{z}} + \epsilon_2 \hat{\mathbf{x}}) \chi_j^\dagger(2\mathbf{r} + \epsilon_1 \hat{\mathbf{z}} + \epsilon_2 \hat{\mathbf{x}}) [U(2\mathbf{r} + \epsilon_1 \hat{\mathbf{z}} + \epsilon_2 \hat{\mathbf{x}}, 2\mathbf{r}) \chi^\dagger(2\mathbf{r})]_k \} |v\rangle. \end{aligned} \quad (6.6)$$

Finally, we write the  $\mathbf{A}_1^-$  state corresponding to the  $\frac{1}{2}^-$  nucleon:

$$\begin{aligned} & \frac{1}{8} \sum_{\mathbf{r}} \sum_{\epsilon_1, \epsilon_2, \epsilon_3} \epsilon_1 \epsilon_2 \epsilon_3 \epsilon_{ijk} [U(2\mathbf{r} + \epsilon_1 \hat{\mathbf{x}} + \epsilon_2 \hat{\mathbf{y}} + \epsilon_3 \hat{\mathbf{z}}, 2\mathbf{r} + \epsilon_1 \hat{\mathbf{x}} + \epsilon_2 \hat{\mathbf{y}}) \chi^\dagger(2\mathbf{r} + \epsilon_1 \hat{\mathbf{x}} + \epsilon_2 \hat{\mathbf{y}})]_i \\ & \quad \times [U(2\mathbf{r} + \epsilon_1 \hat{\mathbf{x}} + \epsilon_2 \hat{\mathbf{y}} + \epsilon_3 \hat{\mathbf{z}}, 2\mathbf{r} + \epsilon_2 \hat{\mathbf{y}} + \epsilon_3 \hat{\mathbf{z}}) \chi^\dagger(2\mathbf{r} + \epsilon_2 \hat{\mathbf{y}} + \epsilon_3 \hat{\mathbf{z}})]_j \\ & \quad \times [U(2\mathbf{r} + \epsilon_1 \hat{\mathbf{x}} + \epsilon_2 \hat{\mathbf{y}} + \epsilon_3 \hat{\mathbf{z}}, 2\mathbf{r} + \epsilon_3 \hat{\mathbf{z}} + \epsilon_1 \hat{\mathbf{x}}) \chi^\dagger(2\mathbf{r} + \epsilon_3 \hat{\mathbf{z}} + \epsilon_1 \hat{\mathbf{x}})]_k |v\rangle. \end{aligned} \quad (6.7)$$

Starting from the above  $\mathbf{A}_1$ ,  $\mathbf{A}_2$ , and  $\mathbf{E}$  states, one can obtain the complete 4, 4', and 8 multiplets, respectively, by applying the face-diagonal shifts to the above states.

## VII. THE $t$ EXPANSION

The  $t$  expansion method has been reviewed extensively in the context of pure gauge theories [9,12,13]. Its application to lattice theories with dynamical quarks was de-

TABLE V. Relation between  $G$  irreps and observed particles.

$G$	$SU(2)_{\text{spin}} \times SU(2)_{\text{flavor}}$	Lightest particle	
		$P=+$	$P=-$
4	$(\frac{1}{2}^\pm, \frac{1}{2}), (\frac{3}{2}^\pm, \frac{3}{2}), (\frac{5}{2}^\pm, \frac{3}{2})$	$N(939)$	$N(1535)$
4'	$(\frac{3}{2}^\pm, \frac{3}{2}), (\frac{5}{2}^\pm, \frac{1}{2}), (\frac{5}{2}^\pm, \frac{3}{2})$	$\Delta(1232)$	$N(1675)$
8	$(\frac{3}{2}^\pm, \frac{1}{2}), (\frac{1}{2}^\pm, \frac{3}{2}), (\frac{3}{2}^\pm, \frac{3}{2}), (\frac{5}{2}^\pm, \frac{1}{2}), (\frac{5}{2}^\pm, \frac{3}{2})$	$\Delta(1232)$	$N(1520)$

scribed in Refs. [1,15]. Underlying the  $t$  expansion is the notion that if  $|\psi_0\rangle$  is a state having a finite overlap with the ground state, then the one parameter family of states [12],

$$|\psi_t\rangle = \frac{1}{\langle \psi_0 | e^{-tH} | \psi_0 \rangle} e^{-tH/2} |\psi_0\rangle, \quad (7.1)$$

contracts onto the ground state of  $H$  as  $t \rightarrow \infty$ .

From this it follows that the energy function

$$E_\phi(t) = \frac{\langle \phi | H e^{-tH} | \phi \rangle}{\langle \phi | e^{-tH} | \phi \rangle}, \quad (7.2)$$

where  $|\phi\rangle$  is some hadronic state, tends to the mass of

the lightest particle with the same quantum numbers as  $|\phi\rangle$  in the same limit. Moreover,  $E_\phi(t)$  can be written as

$$E_\phi(t) = \sum_{n=0}^{\infty} \frac{(-t)^n}{n!} \langle H^{n+1} \rangle_\phi^c, \quad (7.3)$$

where the connected matrix elements  $\langle H^{n+1} \rangle_\phi^c$  are defined recursively by [9]

$$\langle H^{n+1} \rangle_\phi^c = \sum_i \langle \phi | H^{n+1} | \phi \rangle - \sum_{p=0}^{n-1} \binom{n}{p} \langle H^{p+1} \rangle_\phi^c \sum_i \langle \phi | H^{n-p} | \phi \rangle, \quad (7.4)$$

where we have utilized translation invariance by singling out a geometrical unit near the origin ( $i=0$ ). After evaluating  $E_\phi(t)$ , we subtract from it the vacuum energy

$E_0(t)$  to obtain a prediction for the mass function  $M_\phi(t)$ . All our physical predictions will be presented in the form of mass ratios which, beyond the crossover region [1], represent the lattice approximation of the continuum theory.

Equations (7.3) and (7.4) lead to an expansion of the function  $M_\phi(t)$  as a power series in the auxiliary variable  $t$ . Exploiting such Taylor series of any  $t$  expansion of an operator  $O(t)$  is done by forming  $D$ -Padé approximants [13] to the series in  $t$  and using them to obtain the asymptotic value of  $O(t)$ . This means approximating the  $t$  derivative of the expression by nondiagonal  $L/M$  Padé approximants which are integrated out to infinity. In order for the integration to work the degrees of the polynomials have to be chosen so that  $M \geq L + 2$ . The number of approximants generated this way is much larger than that of the diagonal approximants that one can generate for the finite series.

### VIII. BARYON MASSES

In the  $4'$  sector, the lightest observed particle is the  $\Delta$ . We have calculated this state using Eq. (6.4), obtaining the following series to the  $H^7$  order:

$$\begin{aligned} M_{\Delta_4'}(t, y) = & \frac{4}{y} + \frac{15y}{4}t - \frac{7y}{2}t^2 + \frac{1}{576}(-3859y^3 + 896y)t^3 + \frac{1}{432}(255y^5 + 5754y^3 - 224y)t^4 \\ & + \frac{1}{207360}(62910y^7 + 1753941y^5 - 3150144y^3 + 28672y)t^5 \\ & + \frac{1}{933120}(61425y^9 - 3111003y^7 - 21042669y^5 + 13597856y^3 - 28672y)t^6 + O(t^7). \end{aligned} \quad (8.1)$$

Next we calculate the  $J^P = \frac{1}{2}^-$  nucleon, designated as  $N^*$ , by using Eq. (6.7). Its mass series to the  $H^7$  order is

$$\begin{aligned} M_{N^*}(t, y) = & \frac{4}{y} + \frac{21y}{4}t - \frac{9y}{2}t^2 + \frac{1}{576}(-5875y^3 + 1152y)t^3 + \frac{1}{144}(85y^5 + 2434y^3 - 96y)t^4 \\ & + \frac{1}{69120}(15210y^7 + 1075057y^5 - 1227456y^3 + 12288y)t^5 \\ & + \frac{1}{933120}(16065y^9 - 3338622y^7 - 32650635y^5 + 14812064y^3 - 36864y)t^6 + O(t^7). \end{aligned} \quad (8.2)$$

The computation of extended baryon states such as Eqs. (6.4) and (6.7) possesses new features of complexity. The state  $\Delta_4'$  can be propagated on the lattice only by applying to its moments of the Hamiltonian equal to, or higher than,  $H^8$ . On the other hand, we cannot reach orders higher than  $H^7$  due to the vast growth of the number of connected diagrams. Thus, we expect that the mass ratios involving such states will display poorer scaling behavior than the ratios of lowest-lying hadrons previously calculated. We also note that the computation of the states that correspond to the  $\Delta$  particle in the 8 sector, i.e., Eqs. (6.5) and (6.6), involves more than a thousand connected diagrams already in the  $H^7$  order. These states are at present beyond our calculational ability.

In Fig. 1 we display the ratios of the  $N^*$  to the  $\Delta_4'$ . The solid, dotted, and dot-dashed curves correspond to the 0/3, 0/4, and 0/5  $D$ -Padé approximants, respectively.

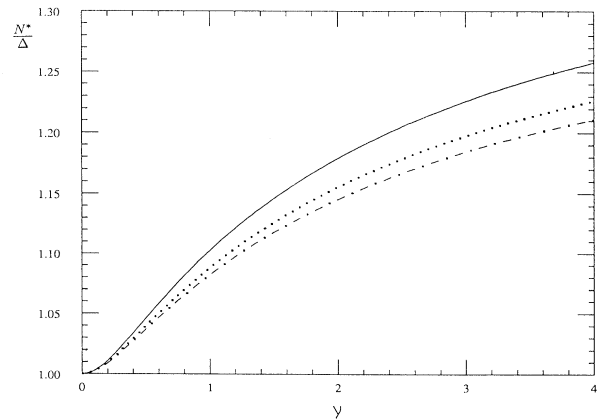


FIG. 1.  $N^*$  to  $\Delta_4'$  mass ratios. The solid, dotted, and dot-dashed lines are the 0/3, 0/4, and 0/5 approximants, respectively.

In general, all our mass ratios are of order  $t^6$ , and thus we can plot only the 0/2, 0/3, 0/4, 0/5, 1/3, and 1/4  $D$ -Padé approximants. Usually some of the approximants have singularities or vary strongly. In all figures that follow, we will display only those  $D$ -Padé approximants which are not plagued by these features, and which are more or less consistent with one another. In all our mass ratios, we expect to find the physical result just beyond the crossover region [1], i.e., near  $y \sim 2$ . The ratio in Fig. 1 starts at 1 in the strong-coupling limit, since both states are composed of three gauge links. Extrapolating toward the weak-coupling region, we observe that the approximants do not reflect any scaling tendency, although the  $N^*$  becomes heavier than the  $\Delta$ , as it should. We associate this lack of scaling with the extended nature of these baryons explained earlier.

After evaluating  $D$ -Padé approximants of various mass ratios, we might attempt to plot ratios of any two such ratios. Based on previous experience of applying the  $t$  expansion to the pure gauge theory [9], we hope to extract new information this way. Indeed, in Fig. 2 we display the ratios between the two mass ratios  $N/\Delta_4$  and  $N/N^*$ , thus obtaining a better estimate for the  $N^*/\Delta_4$  ratio. The plots in Fig. 2 do stabilize near  $y \sim 2$  on a value in the range of 1.26–1.3, in agreement with observed masses.

We note, however, that although the ratio between the  $N^*$  and the  $\Delta$  masses turns out to be of the right magnitude, each of these masses turns out to be too high, as we shall soon find out by looking at mass ratios between any of these extended baryons and lowest-lying hadrons previously calculated. It is interesting to calculate also the  $\Delta$  mass in another lattice multiplet and to check whether the two  $\Delta$  multiplets coincide in the continuum limit. Unfortunately, the  $\Delta$  in the 8 sector is too difficult to compute. In the 4 sector, the  $\Delta$  is seen to be the first excitation and can, in principle, be derived from the lowest-lying state of this sector, the nucleon, by a standard procedure in the  $t$  expansion [14]. The expression obtained this way for the next level is volume dependent,

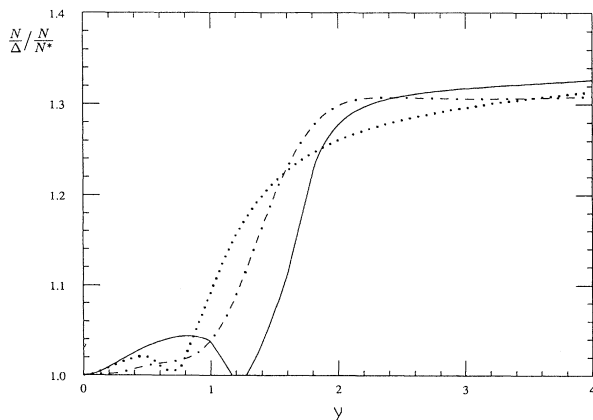


FIG. 2. Ratio between the  $N/\Delta$  and the  $N/N^*$  mass ratios. The solid, dotted, and dot-dashed lines are ratios of the 0/4, 0/5, and 1/4  $D$ -Padé, respectively.

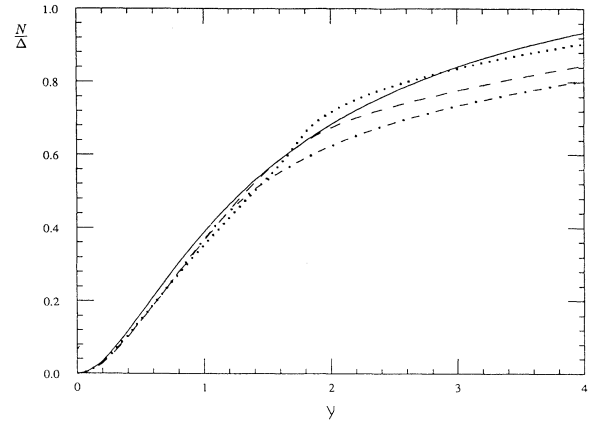


FIG. 3. Mass ratios between the nucleon to the  $\Delta_4$ . The solid, dotted, dot-dashed, and dashed lines are the 0/3, 0/4, 0/5, and 1/4 approximants, respectively.

hence we have tried to manipulate it by means of the exp-fit method [9], namely, to fit the norm function  $\langle \psi_0 | e^{-th} | \psi_0 \rangle$  with a finite series of decreasing exponentials, but we did not succeed to extract from it any meaningful results.

Next, we study the scaling ratios between the nucleon and our extended baryons. In Figs. 3 and 4 we plot the ratios of the nucleon with the  $\Delta$  and the  $N^*$  approximants, respectively. Again, the curves displayed do not exhibit a clear scaling behavior, especially in case of the  $\Delta$  state. Attempting to read the value of these ratios near  $y \sim 2$ , we obtain a value in the range of 0.48–0.58 for the  $N^*$  and 0.61–0.66 for the  $\Delta$ . These values are too low and correspond to a  $\Delta$  mass in the range of 1420–1540 MeV, and an  $N^*$  mass in the range of 1620–1960 MeV.

Figures 5 and 6 show the mass ratios of the  $\omega$  meson to the  $\Delta$  and the  $N^*$ , respectively. Again, the ratio connected with the  $N^*$  reflects a better tendency for scaling. Therefore, in Fig. 7 we plot the ratios between the nucleon to  $\Delta$  ratio and the nucleon to  $\omega$  ratio. This way we

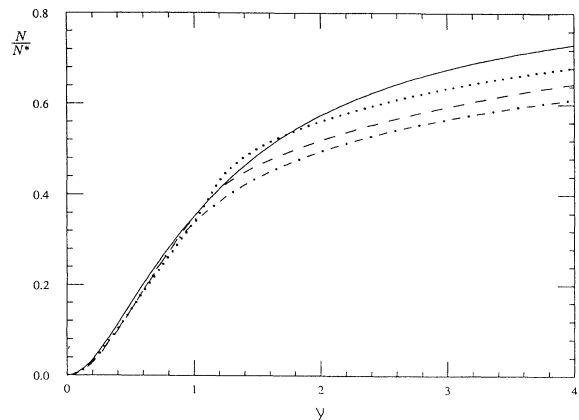


FIG. 4. Nucleon to  $N^*$  mass ratios. The solid, dotted, dot-dashed, and dashed lines are the 0/3, 0/4, 0/5, and 1/4  $D$ -Padé, respectively.



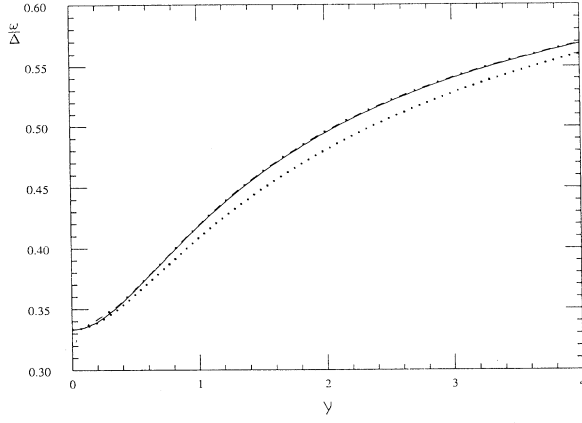


FIG. 5. Mass ratios between the  $\omega$  and the  $\Delta_{4+}$ . Shown are the 0/3 (solid line), 0/4 (dotted line), and 1/4 (dot-dashed line) approximants.

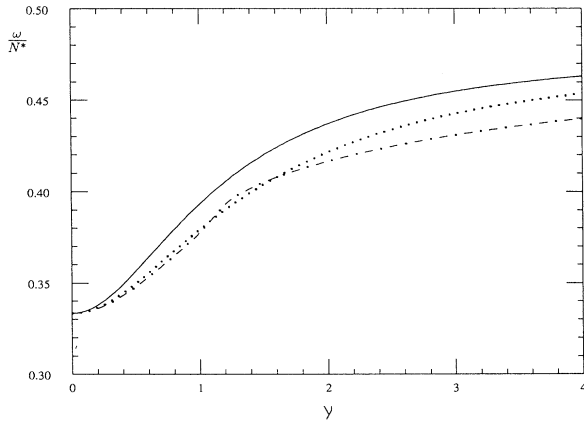


FIG. 6.  $\omega$  to  $N^*$  mass ratios. The solid, dotted, and dot-dashed lines are the 0/2, 0/3, and 0/4 approximants, respectively.

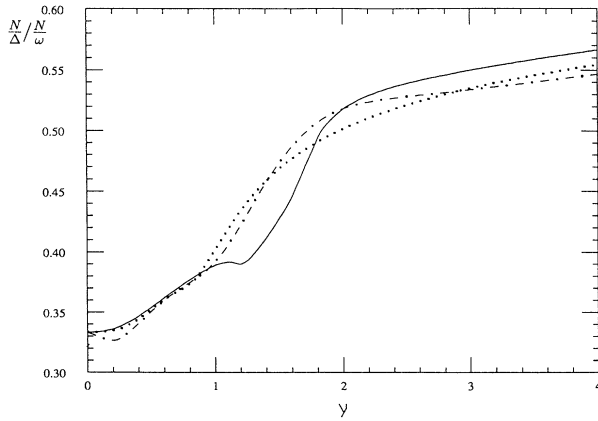


FIG. 7. Ratio between the  $N/\Delta$  and the  $N/\omega$  mass ratios. The solid, dotted, dot-dashed, and dashed lines are ratios of the 0/3, 0/4, 0/5, and 1/4 approximants, respectively.

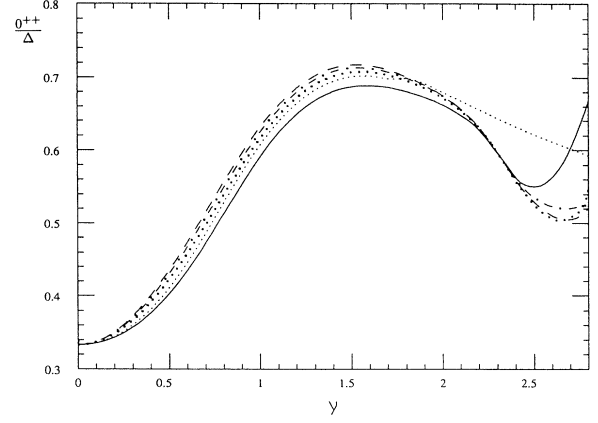


FIG. 8.  $D$ -Padé approximants of the mass ratios between the scalar and the  $\Delta_{4+}$ . The approximants shown are the 0/2 (solid line), 0/3 (dotted line), 0/4 (dot-dashed line), 0/5 (dashed line), and 1/4 (highest dotted line in the high  $\gamma$  region).

obtain a better estimate for the  $\omega$  to  $\Delta$  mass ratios. The plots in Fig. 7 almost stabilize to a clear asymptotic behavior and near  $\gamma \sim 2$  we read the ratio to be in the range 0.5–0.52. From Fig. 6 we read in the same way a value in the range 0.415–0.435 for the  $\omega$  to the  $N^*$  mass ratios. All these figures are consistent with one another, and indicate a value for the  $\Delta$  and  $N^*$  masses which are about 25% higher than their experimental value.

Finally, in Figs. 8 and 9 we display the mass ratios between the  $0^{++}$  to the  $\Delta$  and  $N^*$ , respectively. The peak-shaped curves in these figures are characteristic of mass ratios connected to the scalar state [1]. Although these curves do not settle onto a clear asymptotic trend, we may estimate from the peak at the crossover region ( $\gamma \sim 1.5$ – $1.8$ ) a ratio of 0.66–0.72 in the  $\Delta$  case, and a ratio of 0.57–0.63 for the  $N^*$ .

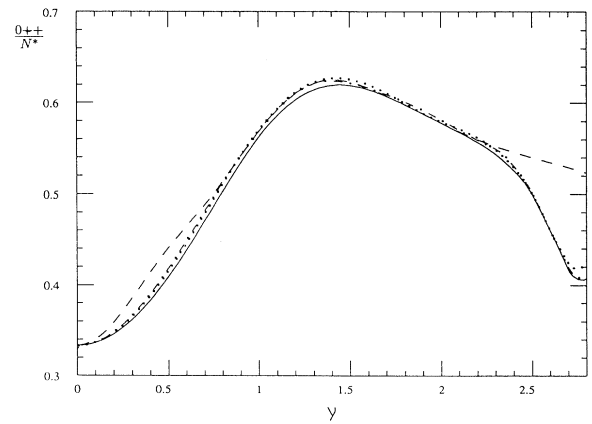


FIG. 9.  $D$ -Padé approximants of the mass ratios between the scalar and the  $N^*$ . The approximants shown are the 0/3 (solid line), 0/4 (dotted line), 0/5 (dot-dashed line), and 1/4 (dashed line).

### IX. DISCUSSION

We use a diagrammatic Hamiltonian approach, the  $t$  expansion, within the Kogut-Susskind formulation. For the first time this is applied to baryons which are not pointlike objects on the lattice.

The calculation of these extended objects is cumbersome. Moreover, such states need higher-order expansions than the lowest-lying hadrons in order to propagate on the lattice. This fact may explain why we obtained too high baryon masses. Nonetheless, we found a consistent picture of the baryons' hierarchy, namely,

$$M(\frac{1}{2}^+, \frac{1}{2}) < M(\frac{3}{2}^+, \frac{3}{2}) < M(\frac{1}{2}^-, \frac{1}{2}) .$$

It is interesting to note that although each of the mass ratios in Figs. 1, 3, and 4, namely, the  $N^*/\Delta$ ,  $N/\Delta$ , and  $N/N^*$  mass ratios, do not reflect any scaling tendency, the ratio between the  $N/\Delta$  and the  $N/N^*$  mass ratios settles onto a clear asymptotic trend in Fig. 2. Moreover, it predicts the correct value for the  $N^*/\Delta$  mass ratio. This is in accordance with our working hypothesis, which is to plot all possible mass ratios but to regard as reliable only those plots which show scaling behavior. The existence of scaling, for us, is an indication of the correct-

ness of the result.

Comparing our method with the standard Lagrangian approach, we note that no Monte Carlo simulations were done within the Kogut-Susskind formulation for baryons heavier than the nucleon, with fully dynamical quarks. Also, for Wilson valence quarks the nucleon- $\Delta$  mass splitting is too small. We find the same mass splitting to be too large. Hopefully one can find a better way to generate all relevant connected graphs, and thus continue our calculation to higher orders. This should improve the results for baryons which are extended objects.

In this work we have concentrated solely on the baryonic spectrum. We can apply the  $t$  expansion to explore the mesonic picture of the Kogut-Susskind model of two flavors as well. In particular, one can investigate mesons composed of one heavy quark and one light quark, which have recently been under extensive study. We hope to report on this subject in a forthcoming paper.

### ACKNOWLEDGMENTS

I am indebted to D. Horn, G. Lana, and M. Marcu for very helpful discussions.

- 
- [1] D. Horn and D. Schreiber, Phys. Rev. D **47**, 2081 (1993).
  - [2] T. Jolicoeur and A. Morel, Nucl. Phys. **B262**, 627 (1985).
  - [3] M. Golterman and J. Smit, Nucl. Phys. **B255**, 328 (1985).
  - [4] M. Golterman, Nucl. Phys. **B273**, 663 (1986).
  - [5] J. B. Kogut and L. Susskind, Phys. Rev. D **11**, 395 (1975).
  - [6] L. Susskind, Phys. Rev. D **16**, 3031 (1977).
  - [7] L. Susskind, in *Weak and Electromagnetic Interactions at High Energy*, Proceedings of the Les Houches Summer School, Les Houches, France, 1976, edited by R. Balian and C. H. Llewellyn Smith (North-Holland, Amsterdam, 1977).
  - [8] T. Banks *et al.*, Phys. Rev. D **15**, 1111 (1977).
  - [9] D. Horn, Int. J. Mod. Phys. A **4**, 2147 (1989).
  - [10] C. van den Doel and J. Smit, Nucl. Phys. **B228**, 122 (1983).
  - [11] R. C. Johnson, Phys. Lett. **114B**, 147 (1982).
  - [12] D. Horn and M. Weinstein, Phys. Rev. D **30**, 1256 (1984).
  - [13] D. Horn, M. Karliner, and M. Weinstein, Phys. Rev. D **31**, 2589 (1985).
  - [14] D. Horn, in *From SU(3) to Gravity*, edited by E. Gotsman and G. Tauber (Cambridge University Press, Cambridge, England, 1985).
  - [15] A. Krasnitz and E. G. Klepfish, Phys. Rev. D **37**, 2300 (1988).